CONTINUOUS INDUCTION WELDING OF THERMOPLASTIC ADHERENTS USING MAGNETIC SUSCEPTORS

Martin, R. G.[1], Johansson, C.[2], Tavares, J. R.[3] and Dubé, M.[1]*
[1] CREPEC, Mechanical Engineering, École de Technologie Supérieure (ETS), Montréal, Canada
[2] RISE Research Institutes of Sweden, Göteborg, Sweden
[3] CREPEC, Chemical Engineering, Polytechnique Montréal, Montréal, Canada
* Corresponding author (martine.dube@etsmtl.ca)

Keywords: *Induction welding, Magnetic susceptors, Thermoplastic polymers*

1 INTRODUCTION

Thermoplastic composites are increasingly used in the aerospace industry, mainly because of their ability to be reprocessed, their short process cycle time and their potential to be repaired. They also typically exhibit higher fracture toughness than commonly used thermoset composites such as epoxy systems. Thermoplastic composites joining can be done using adhesives or mechanical fasteners, but these techniques present limitations. The use of adhesives requires extensive surface preparation such as plasma pre-treatments to achieve satisfying results, due to the polyolefins' low surface energy [1]. On the other hand, the presence of fasteners can induce delamination or deconsolidation as the holes create stress concentration points. An alternative is to turn to fusion bonding, or welding, which relies on the ability of the thermoplastic materials to melt – or soften in the case of an amorphous polymer – and be reprocessed ([2], [3]). At the joining temperature, the polymer chains have enough mobility to migrate through the interface and create a bond, in a process called interface healing ([4]–[6]). The created bond is then consolidated under pressure. Three main fusion bonding techniques are currently used in the aerospace industry: ultrasonic, resistance and induction welding ([2], [7]).

In this paper, the latter is used as the joining technique. Induction welding is a fusion bonding process using a magnetic field as the energy source. A material called susceptor is located at the joining interface and can dissipate heat in the presence of an alternating magnetic field. The heat can be dissipated through the induction of eddy currents in electrically-conductive material or, as it is the case in this work, through hysteresis losses in ferromagnetic materials ([8]–[14]). When magnetic materials are subjected to a time-varying magnetic field, they are magnetized in alternating directions following the magnetic field lines. During this process, a fraction of the received magnetic energy is released into heat, the amount of which is dependent on the material's magnetic hysteresis and is therefore called hysteresis losses ([15], [16]). This energy, categorized as thermal losses in other processes, is used in induction welding to melt the surrounding thermoplastic polymer in the bonding area.

The goal of this paper if to assess the feasibility of the use of magnetic susceptor materials relying on hysteresis losses by producing welded single lap-shear specimens and characterize their mechanical performance.

2 MATERIALS AND METHODS

2.1 Magnetic susceptor

Magnetic susceptors relying on magnetic hysteresis losses are prepared by mixing magnetic particles with a thermoplastic compatible with the parts to be welded. Here, the selected polymer is polypropylene (PP), which is a semi-crystalline thermoplastic. Previous work done by the authors showed which magnetic particles is adapted to produce a magnetic susceptor depending on the used thermoplastic polymer [17]. In the case of PP, the most suitable material among the tested particles was Ni. PP pellets (grade 1104A from Pinnacle Polymers) present a density of 900kg/m^3 and a specific heat capacity of 1970J/(kg·K). The melting point of this material is around 170°C. Ni particles (supplied by Sigma-Aldrich) have an average diameter of 5μm, a density of 8900kg/m^3 and a specific heat capacity of 443J/(kg·K). The Curie temperature of Ni, i.e. the temperature above which the material loses its ferromagnetic properties, is 358°C [9].

PP pellets and Ni particles are mixed using an internal mixer (HAAKE^{TM} Rheomix OS 1010) at 210°C under air atmosphere. The PP pellets are first introduced for 5min to melt them. The Ni particles are then added and mixed with the polymer for another 5min to ensure good spatial distribution. The resulting PP/Ni material is then shredded into pellets and pressed using a hot press at 210°C for 5min to form a 0.75mm-thick film. This film is then cut into long bands of 150mm x 12.7mm that will be used as the susceptor during the welding step.

2.2 Adherents

PP adherents are cut into 150mm x 100mm plates from large sheets (supplied by McMaster-Carr) with a thickness of 2.4mm. Adherents are used as received, without applying any specific surface preparation treatment.

2.3 Induction welding setup

A continuous induction welding setup, presented in Figure 1, is used to join the adherents. The power supply of the induction welding setup is a generator Ambrell EASYHEAT 10kW. A water-cooled copper hairpin coil equipped with a Ferrotron 559H field concentrator is used to generate the magnetic field. In single lap-shear (SLS) configuration, samples are placed on a wooden support mounted on a liner motor, allowing for a lateral displacement perpendicularly to the induction coil axis. Next to the coil, a pressure roller applies compaction force on the overlapping area of the samples after they passed under the coil to ensure bonding. The overlap is length kept fixed at 12.7mm.
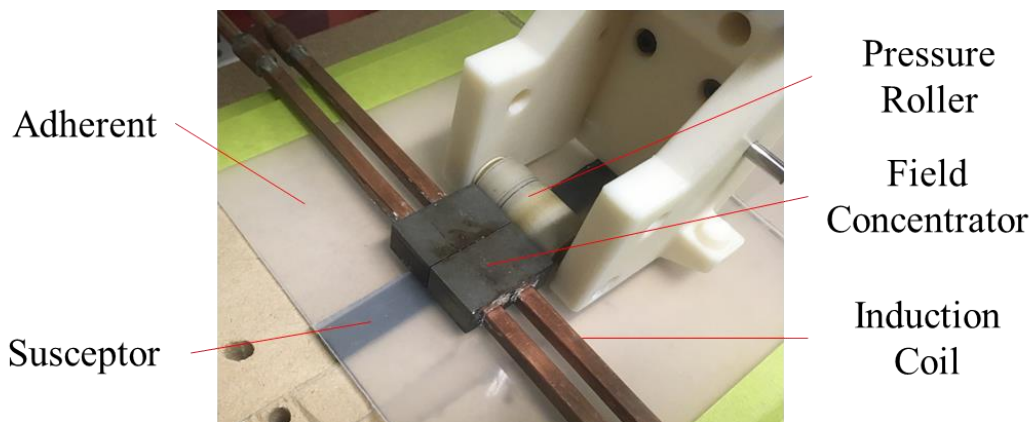

Figure 1 – Induction welding setup in SLS configuration, using a hairpin coil equipped with a magnetic field concentrator

2.4 Experimental parameters

Various experimental parameters can be tuned during welding, such as the coupling distance (between the induction coil and the susceptor film), the magnetic field intensity (controlled by the coil geometry and the applied current), the welding speed (linear motion of the table) and welding force (applied by the pressure roller). In this work, the coupling distance is fixed at 5mm and the applied current at 600A, leading to a maximum magnetic field amplitude of 27.5kA/m. Adherents are welded using PP/Ni susceptor bands with a fixed nickel volume fraction of 10%. Under these conditions, the initial heating rate of the susceptor is predicted to be around 15°C/s, which was confirmed experimentally [17]. The welding force is varied between 50, 100 and 150N and the welding speed between 0.8 and 1.0 mm/s (Table 1).

Table 1 - PP samples name and welding parameters

Sample Name	Welding force [N]	Welding speed [mm/s]
PP-100/0.6	100	0.6
PP-50/0.8	50	0.8
PP-100/0.8	100	0.8
PP-150/0.8	150	0.8
PP-50/1	50	1.0
PP-100/1	100	1.0
PP-150/1	150	1.0

After welding, joined plates are cut using a ribbon saw perpendicularly to the weld line into 25mm-wide SLS specimens. Five specimens are cut from each welded plate. Tensile tests are conducted at room temperature in ambient air conditions following the ASTM D3163 standard, designed for adhesively bonded plastic joints. The speed of the tensile test machine crosshead is fixed at 13mm/s, as per the standard. No conditioning is performed on the specimens before testing them.

2.5 Microscopy analysis

One portion of each welded sample is cut out and the transverse surface is polished using sandpapers of grade 300, 600 and 1200. Then, the bond line profile of the welded samples is observed using a Nikon Eclipse MA100N optical microscope. The thickness of the susceptor layer after welding is reported.

2.6 Failure mode

After the mechanical tests, fractured specimens are visually inspected to define which was the dominant failure mechanism. The failure can be either adhesive (failure between the susceptor layer and the adherent), cohesive (inside the susceptor layer, leading to the presence of susceptor on both sides of the specimen) or occur inside the adherent.

3 RESULTS

3.1 Mechanical tests

SLS test results are presented in Figure 2. The presented value for each sample is the average shear strength of five tested specimens, which is calculated by dividing the force at break by the joining surface area (specimen width multiplied by overlap length). In the current SLS geometry, this area is approximately 318mm^2. The error bars correspond to the standard deviation calculated on the five specimens. The highest average shear strength is reached for samples PP-100/0.8 and PP-150/0.8. The welding speed was low enough to allow time for the susceptor to heat up and melt the surrounding PP, which resulted in a strong bonding, but fast enough to prevent material deformation (as observed at 0.6mm/s, Figure 3). Unexpectedly, the measured average shear strength for sample PP-100/0.6 is lower, although this variation is within the standard deviation. In general, samples welded at 1mm/s (PP-50/1, PP-100/1 and PP-150/1) resulted in lower shear strength. This means that the susceptor could not reach a sufficiently high temperature to provide mobility to the polymeric chain to heal the joining interface. However, increasing the welding force does seem to compensate partially this effect. The importance of applying a large enough force during welding also appears on sample PP-50/0.8, in which the shear strength is low even though the speed was sufficient under larger forces (100N in PP-100/0.8 and 150N in PP-150/0.8). One should keep in mind that increasing the welding force too much will induce a more important weld line thickness reduction, which could also affect the mechanical properties.
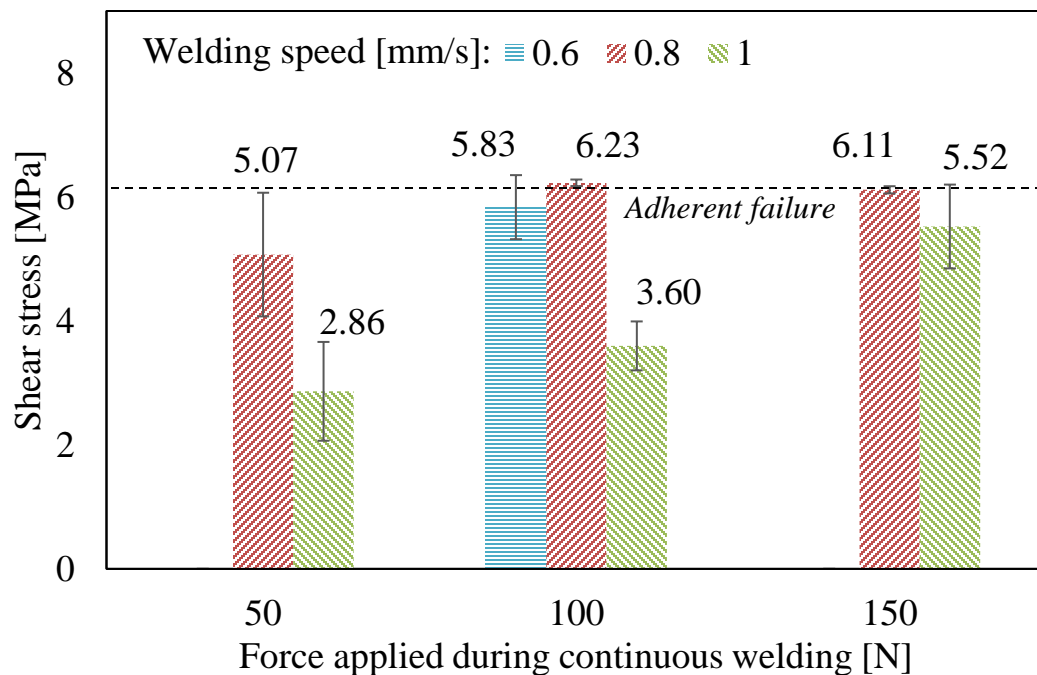

Figure 2 – SLS mechanical tests results. The average value for each sample is reported on the figure. The black dashed line corresponds to the approximate shear stress at which the adherent failed during the experiments.
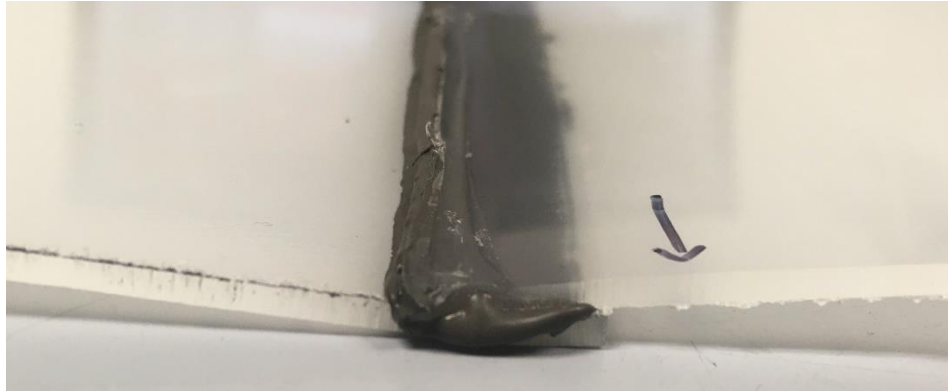
Figure 3 – Bending observed when over-heating sample PP-100/0.6 during welding. A large quantity of the susceptor material (in black) has flowed out of the bonding area and the PP adherent is deformed.

3.2 Fracture analysis

All the fractured specimens are presented in Figure 4 and their main failure modes are summarized in Table 2. Samples PP-100/0.6, PP-100/0.8 and PP-150/0.8 that presented the highest shear strength all exhibit adherent failure, meaning that the failure occurred inside the adherent next to the bonding area for all the tested specimens. The measured strength must therefore not be considered as the joint shear strength, as the weld resisted the applied force. It can only be concluded that the weld was stronger than the measured value. For PP-100/0.6, the obtained value is slightly lower and more variable than for PP-100/0.8 and PP-150/0.8, maybe due to the adherent deformation due to overheating, leading to non-homogeneous adherent thickness and to a lower average strength (although this might not be significant as the difference is covered by the standard deviation). Sample PP-50/0.8 exhibits cohesive failure in some specimens, highlighting the importance of applying the right force to ensure a proper contact and healing between the adherents. The variability of the mechanical results is also visible as the failure occurred differently in all specimens. In sample PP-150/1, more cohesive failure is observed, confirming the previously made observation that increasing the welding force can partially compensate for a higher welding speed. However, in that case, it is still not enough to reach a consistent adherent failure mode like in the best performing samples. The higher force can also cause susceptor to flow out of the bonding region, leading to lower mechanical performance.
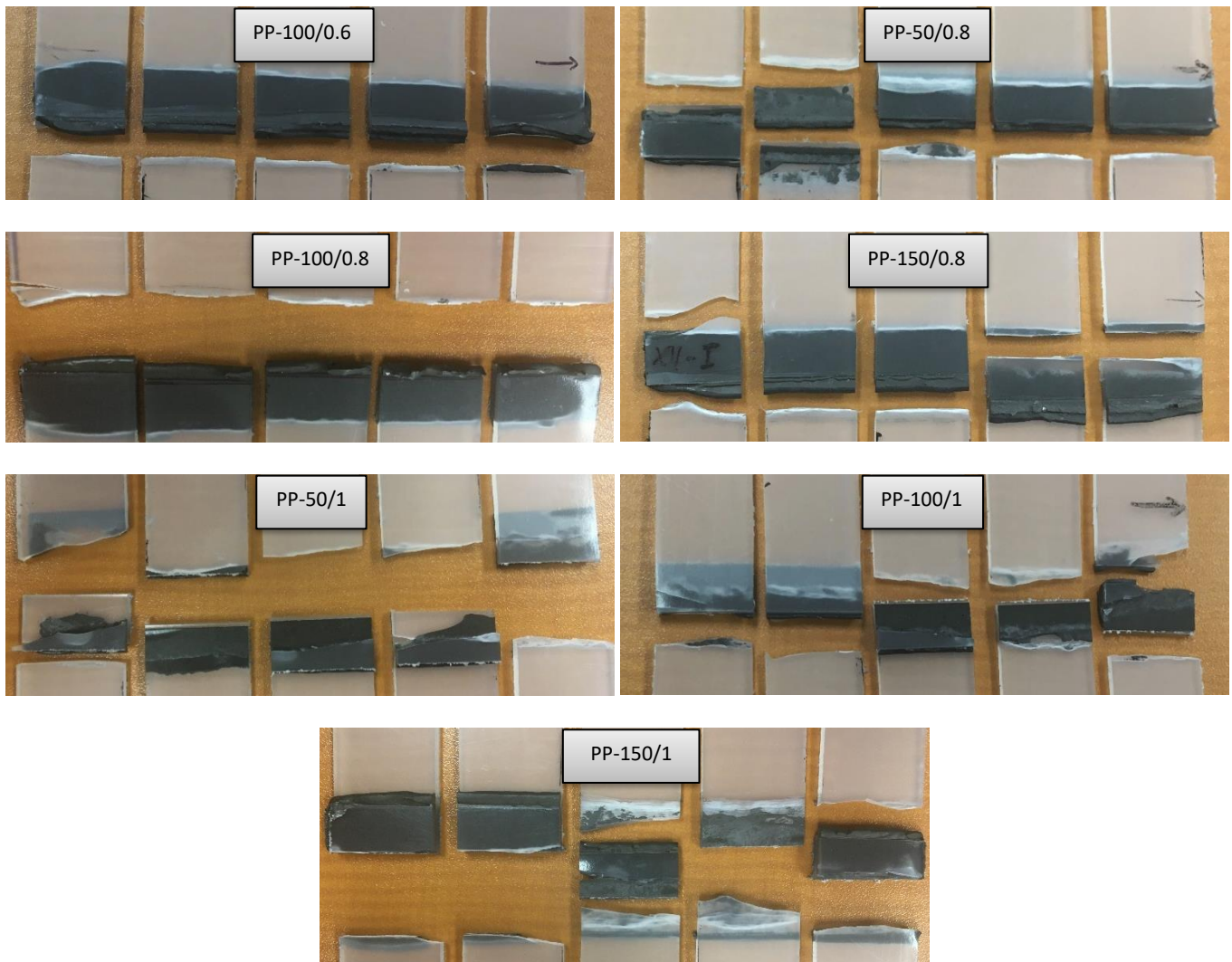
Figure 4 – Fractured SLS specimens.

Table 2 - PP specimens dominant failure mode during tensile test in SLS configuration

Sample Name	Dominant failure Mode
PP-100/0.6	100% adherent failure
PP-50/0.8	80% adherent failure, 20% cohesive failure
PP-100/0.8	100% adherent failure
PP-150/0.8	100% adherent failure
PP-50/1	10% adherent failure, 90% adhesive failure
PP-100/1	30% adherent failure, 70% adhesive failure
PP-150/1	60% adherent failure, 40% cohesive failure

3.3 Weld profile

Microscope observation of the welded bond line allows measuring the susceptor thickness after welding (Figure 5). The average thickness based on three measurements made on the welding line is reported in

Table 3. Sample PP-100/0.6 and PP-100/0.8, which obtained the best mechanical results showed an average thickness of 129μm and 216μm, respectively, compared to the initial thickness of approximately 750μm. Thinner weld lines were observed in samples PP-150/0.8 and PP-150/1, due to the largest welding force (150N), which led to lower mechanical performance. In sample PP-150/0.8, the susceptor was completely pushed away under pressure (right picture, fourth row on Figure 5). Even though the mechanical properties are not affected by the reduction in bond line thickness, it could be minimized to avoid wasting susceptor material as long as the performance is acceptable. Therefore, in the case of a speed of 0.8mm/s, the force can be limited to 100N.

In sample PP-150/1, cohesive failure might have been caused by the thin layer of susceptor remaining at the weld line. In sample PP-100/1 and PP-50/1, the susceptor layer is still thick, showing that the maximum temperature reached during welding was too low, as the susceptor did not deform a lot. Finally, for sample PP-50/0.8, the low performance cannot be attributed to an insufficient speed, as 0.8mm/s provided the best mechanical results. It can therefore be concluded that a welding force of 50N is not sufficient to produce a strong weld. These observations point out to the conclusion that 100N is the correct amount of force to apply to weld PP with the current setup.

It is also worth noting on Figure 5 that the particles dispersion inside the susceptor layer seems to be good. Visually, there are no major agglomerations and no regions with few to no particles. No porosities are observed inside the susceptor layer, which is also necessary to obtain good mechanical properties. This shows that the technique used to mix and prepare the susceptor is appropriate for PP/Ni systems.

Table 3 - PP samples susceptor layer thickness after welding

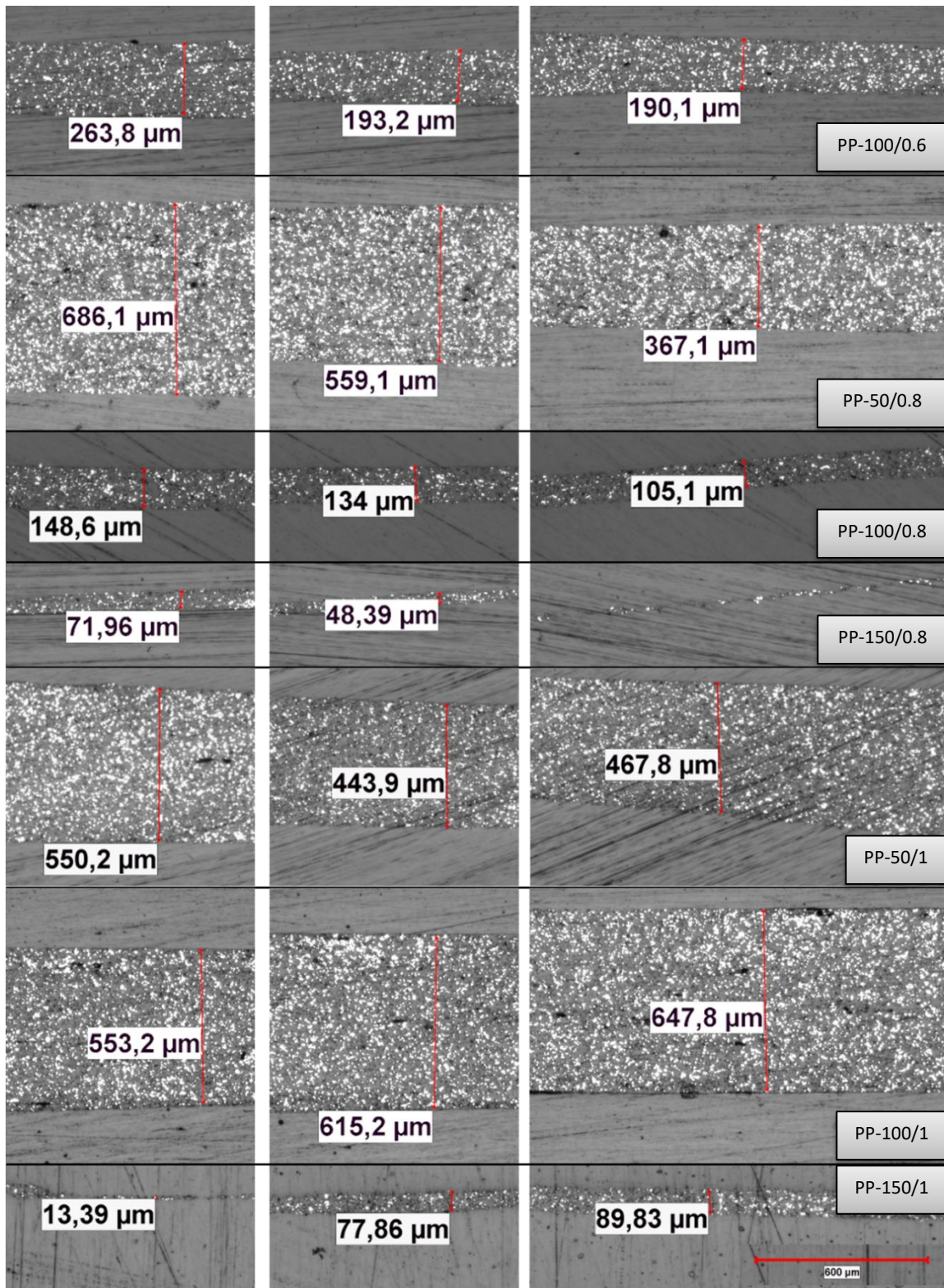| Sample Name	Susceptor thickness after welding [μm]
Before welding	**750**
PP-100/0.6	216
PP-50/0.8	537
PP-100/0.8	129
PP-150/0.8	40
PP-50/1	487
PP-100/1	605
PP-150/1	60

Figure 5 - PP samples welded bond line. The red arrows indicate the location of the thickness measurement and the white dots are the nickel particles distributed in the susceptor layer.

4   CONCLUSION

The results presented in this paper show that using susceptors based on hysteresis losses to perform induction welding of thermoplastic materials is possible. The mixing technique produced homogeneous susceptors with good particles distribution and no porosities. The mechanical tests showed the importance of the welding speed. A too fast welding speed does not give enough time for the susceptor material to heat up, melt the surrounding thermoplastic and heal the interface. On the other hand, there is a risk of over-heating when going too slow. This leads to deformed joints and large susceptor outflow. A high welding speed can be partially compensated by increasing the welding force, which leads to better mechanical performance. A good balance must be found between these welding parameters to produce stronger and repeatable welds. In this specific case, the optimal parameters to continuously weld PP adherents by induction using PP/Ni-10%vol susceptor are a welding speed of 0.8mm/s and a welding force of 100N.

Future work will include transferring this technique to high performance thermoplastics and thermoplastic composites, where the stronger adherents will prevent the adherent failure, giving the opportunity to better observe and characterize the actual weld strength. An alternate way to prevent the adherent failure is to increase its thickness.

ACKNOWLEDGEMENTS

REFERENCES

[1]   C. Mandolfino, "Polypropylene surface modification by low pressure plasma to increase adhesive bonding: Effect of process parameters," *Surf. Coat. Technol.*, vol. 366, pp. 331–337, May 2019, doi: 10.1016/j.surfcoat.2019.03.047.

[2]   A. Yousefpour, M. Hojjati, and J.-P. Immarigeon, "Fusion Bonding/Welding of Thermoplastic Composites," *J. Thermoplast. Compos. Mater.*, vol. 17, no. 4, pp. 303–341, Jul. 2004, doi: 10.1177/0892705704045187.

[3]   C. Ageorges, L. Ye, and M. Hou, "Advances in fusion bonding techniques for joining thermoplastic matrix composites: A review," *Compos. Part Appl. Sci. Manuf.*, vol. 32, pp. 839–857, Jun. 2001, doi: 10.1016/S1359-835X(00)00166-4.

[4]   L. J. Bastien and J. W. Gillespie, "A non-isothermal healing model for strength and toughness of fusion bonded joints of amorphous thermoplastics," *Polym. Eng. Sci.*, vol. 31, no. 24, pp. 1720–1730, 1991, doi: 10.1002/pen.760312406.

[5]   C. A. Butler, R. L. Mccullough, R. Pitchumani, and J. W. Gillespie, "An Analysis of Mechanisms Governing Fusion Bonding of Thermoplastic Composites," *J. Thermoplast. Compos. Mater.*, vol. 11, no. 4, pp. 338–363, Jul. 1998, doi: 10.1177/089270579801100404.

[6] R. P. Wool, B.-L. Yuan, and O. J. McGarel, "Welding of polymer interfaces," *Polym. Eng. Sci.*, vol. 29, no. 19, pp. 1340–1367, 1989, doi: 10.1002/pen.760291906.

[7] I. F. Villegas, L. Moser, A. Yousefpour, P. Mitschang, and H. E. Bersee, "Process and performance evaluation of ultrasonic, induction and resistance welding of advanced thermoplastic composites," *J. Thermoplast. Compos. Mater.*, vol. 26, no. 8, pp. 1007–1024, Sep. 2013, doi: 10.1177/0892705712456031.

[8] S. Yarlagadda, B. K. Fink, and J. J. W. Gillespie, "Resistive Susceptor Design for Uniform Heating during Induction Bonding of Composites," *J. Thermoplast. Compos. Mater.*, Aug. 2016, doi: 10.1177/089270579801100403.

[9] T. Bayerl, M. Duhovic, P. Mitschang, and D. Bhattacharyya, "The heating of polymer composites by electromagnetic induction – A review," *Compos. Part Appl. Sci. Manuf.*, vol. 57, pp. 27–40, Feb. 2014, doi: 10.1016/j.compositesa.2013.10.024.

[10] T. J. Ahmed, D. Stavrov, H. E. N. Bersee, and A. Beukers, "Induction welding of thermoplastic composites—an overview," *Compos. Part Appl. Sci. Manuf.*, vol. 37, no. 10, pp. 1638–1651, Oct. 2006, doi: 10.1016/j.compositesa.2005.10.009.

[11] L. Moser, "Experimental Analysis and Modeling of Susceptorless Induction Welding of High-Performance Thermoplastic Polymer Composites," *undefined*, 2012, Accessed: Apr. 03, 2021. [Online]. Available: /paper/Experimental-Analysis-and-Modeling-of-Susceptorless-Moser/f24c3df7520ba247dce7fc9adc0906f6dcd84086

[12] R. Dermanaki Farahani and M. Dubé, "Novel Heating Elements for Induction Welding of Carbon Fiber/Polyphenylene Sulfide Thermoplastic Composites," *Adv. Eng. Mater.*, vol. 19, no. 11, p. e201700294, Jun. 2017, doi: 10.1002/adem.201700294.

[13] R. Dermanaki Farahani, M. Janier, and M. Dubé, "Conductive films of silver nanoparticles as novel susceptors for induction welding of thermoplastic composites," *Nanotechnology*, vol. 29, Jan. 2018, doi: 10.1088/1361-6528/aaa93c.

[14] R. Rudolf, P. Mitschang, and M. Neitzel, "Induction heating of continuous carbon-fibre-reinforced thermoplastics," *Compos. Part -Appl. Sci. Manuf. - COMPOS PART -APPL SCI MANUF*, vol. 31, pp. 1191–1202, Nov. 2000, doi: 10.1016/S1359-835X(00)00094-4.

[15] J. M. D. Coey, *Magnetism and Magnetic Materials*. Cambridge University Press, 2010.

[16] R. G. Martin, C. Johansson, J. R. Tavares, and M. Dubé, "Heating rate prediction for induction welding magnetic susceptors," 36th Technical Conference of the American Society for Composites 2021, 2021, pp. 11–23.

[17] R. G. Martin, C. Johansson, J. R. Tavares, and M. Dubé, "Material Selection Methodology for an Induction Welding Magnetic Susceptor Based on Hysteresis Losses," *Adv. Eng. Mater.*, vol. n/a, no. n/a, p. 2100877, 2021, doi: 10.1002/adem.202100877.